

Morphological influence of ZnO nanostructures and Cu loading for the photodegradation of methyl parathion

A

Thesis submitted

In partial fulfillment of the requirements for the degree of

MASTERS OF SCIENCE

in

CHEMISTRY



Submitted By

SatinderKaur

(Regd. No.:301502032)

UNDER THE SUPERVISION OF

Dr. Satnam Singh

Professor

**SCHOOL OF CHEMISTRY AND BIOCHEMISTRY,
THAPAR UNIVERSITY, PATIALA-147004**

July, 2017

Certificate

This is to certify that the thesis entitled "**Morphological influence of ZnO nanostructures and Cu loading for the photodegradation of methyl parathion**" being submitted by **Ms. Satinder Kaur** in partial fulfillment of the requirements for the award of degree of Master of Science in Chemistry to the School of Chemistry and Biochemistry, Thapar University, Patiala, is a bonafide work carried out by her under my supervision. The contents of this thesis have not been submitted for the award of any other degree or diploma.



(Supervisor)

Dr. Satnam Singh

Professor,

School of Chemistry and Biochemistry,

Thapar University, Patiala - 147004

Candidate's Declaration

I hereby declare that the work being presented in the thesis entitled "**Morphological influence of ZnO nanostructures and Cu loading for the photodegradation of methyl parathion**" in partial fulfillment of the requirements for the award of degree of Master of Science in Chemistry, and being submitted to School of Chemistry & Biochemistry, Thapar University, Patiala, is my own work during the period of January to July 2017, under the supervision of Dr. Satnam Singh. I have not submitted the contents embodied in this thesis for the award of any other degree.

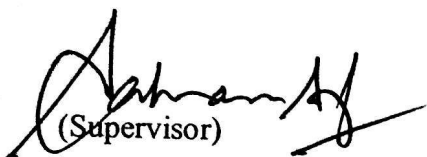
Date: 14/07/2017

Place: Patiala



(Satinder Kaur)

This is to certify the above statement made by Ms. Satinder Kaur is correct and true to the best of my knowledge.



(Supervisor)

Dr. Satnam Singh

Professor,

School of Chemistry and Biochemistry,

Thapar University, Patiala - 147004

ACKNOWLEDGEMENTS

The piece of work would never have been accomplished without the blessings of God and also without the people in my life inspiring, motivating, guiding and accompanying me throughout my dissertation.

I own a deep sense of gratitude to my supervisor **Dr. Satnam Singh**, Professor, School of Chemistry and Biochemistry, Thapar University, Patiala for his keen interest, expert guidance, and motivation during my project work. I am thankful for his valuable suggestions and constructive criticism until the completion of my project.

A special word of appreciation for helpful and encouraging attitude of **Dr. Amjad Ali**, Associate Professor and Head, School of Chemistry and Biochemistry, Thapar University, Patiala and **Dr. Bonamali Pal** and former Head, School of Chemistry and Biochemistry, Thapar University, Patiala for providing necessary facilities during my thesis.

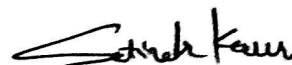
I extend my special thanks to my mentor **Mr. Rayees Ahmad Rather** for his guidance, support, encouragement and suggestions throughout the period.

I extend my special thanks to the PhD Scholars **Ms. Tanushee Basu**, **Ms. Samriti Thakur** and **Mr. Roop Chand Prajapat** for their immense cooperation, timely help and moral support provided by them during the complete span of my project.

I would also like to acknowledge Nitya Chawala , Bhavya Khurana, Nishant Thakur, Bimal Garg for their unfailing support, wishes and continuous encouragement for the successful completion of this thesis.

Words are not enough to express my feelings about my immense gratitude that I owe to my dear Parents for their endless love, blessings and moral support throughout my life. Last but not the least I am thankful to all the persons who helped me directly or indirectly during the tenure of my project work.

Place: Patiala



Satinder Kaur

List of content

Content	Page No
1. Introduction	1-5
1. Literature review	5-8
2. Research gap	9
3. Objective	9
4. Methodology	10-13
5. Results and Discussion	14-26
6. Conclusion	27
7. Reference	28-32
8. Plagiarism Certificate	33

List of abbreviations

°C	Degree Celsius
%	Percent
G	Grams
Mg	Milligram
CB	Conduction band
VB	Valance band
μ	Micro
Nm	Nanometer
SEM	Scanning electron microscope
NP	Nanoparticles
NR	Nanorods like structure
NS	Nanospheres like structure
NF	Nanoflowers like structure
Ppm	Particles per million

List of figures

Figure.1. Solid state UV-Vis absorbance spectra of ZnO and Cu doped ZnO nanoparticles.

Figure.2. X-ray diffraction pattern of ZnO NP and Cu loaded ZnO nanoparticles .

Figure.3. SEM images of ZnO (a and b) Nanoflower like, (c and d) Nanorods like.

Figure.4. SEM images of (e and f) Nanospheres and EDS spectra .

Figure.5. SEM images of Cu-ZnO (a and b) Nanoflower like, (c and d) Nanorods like.

Figure.6. SEM image of (e and f) nanospheres like and EDS spectra.

Figure.7. UV absorbance spectra of degradation of methyl parathion with ZnO NP.

Figure.8. UV absorbance spectra of degradation of methyl parathion with Cu-loaded ZnO NP.

Figure.9. Photodegradation efficiency % with (a) ZnO NP (b) Cu doped ZnO NP.

Figure.10. Time vs concentration graph of photodegradation (a) ZnO NP (b) Cu doped ZnO.

Figure.11. Comparative degradation of pesticide with (a) ZnO NP (b) Cu loaded ZnO NP

Figure.12. GC graph of ZnO NF and Cu-ZnO NP.

Figure.13. CO₂ production with ZnO and Cu-ZnO.

Figure.14. Photodegradation of methyl parathion with ZnO.

Figure.15. Photodegradation of methyl parathion with ZnO.

Abstract

Pesticides accumulation in ecosystem becomes a major concern that causes many health problems. Zinc oxide is a promising photocatalyst for the degradation of pesticides and dyes because of its high stability, low cost and low toxicity. Different shapes of ZnO nanoparticles were prepared and loaded with Cu²⁺ ions. These materials were characterized by XRD, SEM, EDS and diffuse spectroscopy. The photocatalytic degradation of methyl parathion, an organophosphorus pesticide is investigated by different shapes of ZnO and by Cu loaded ZnO nanoparticles. ZnO nanorods gave better catalytic activity than other shapes because of its elongated morphology and with Cu loading its activity is further enhanced. Moreover, among different shapes of the nanocomposites, nanorods exhibited the highest catalytic activity for the photooxidation for methyl parathion (98%) into CO₂ and H₂O.

Introduction

The chemical species which increases or decreases the rate of reaction by association or dissociation of chemical bonds of reactants is known as catalyst.¹ In chemical industry, roughly 90% of the products made by the use of catalytic processes. The term “catalysis” was first discovered by chemist Elizabeth Fulhame which was later used by Berzelius in 1835 to identify a new species capable of promoting the chemical reaction by “catalytic contact”, the catalyst was seen as a specie that was added to reaction mixture to increase the rate of the reaction without being produced or consumed.² From many centuries, catalytic technology has been used like in production of wine by enzyme as catalysts and making of soaps by inorganic catalyst. In 1875, platinum catalyst used for the production of H₂SO₄ on large scale. Various materials like clays, silica and many metal oxides like TiO₂, ZnO, CdS, WO₃, SnO₂, ZnS, CdTe, etc. all have been used as catalyst in nanoscale from many years. But the correct explanation of marvelous catalytic behavior of nanoparticles (NP) still has not been fully understood, may be a reasonable explanation of marvelous catalytic activity is large surface area of NP which directly increase reaction rate. Different morphologies formed are based on the properties of any materials at its nanoscale size which also effect catalytic activity of a material.³⁻⁷ According to thermodynamic, chemical entity which enhance the rate the of attainment of equilibrium but itself remain unchanged is called the catalyst and such reactions are known as catalytic reaction. A catalyst provides different mechanisms which include an alternative transition state which lower the activation energy of reaction than uncatalyzed reactions.

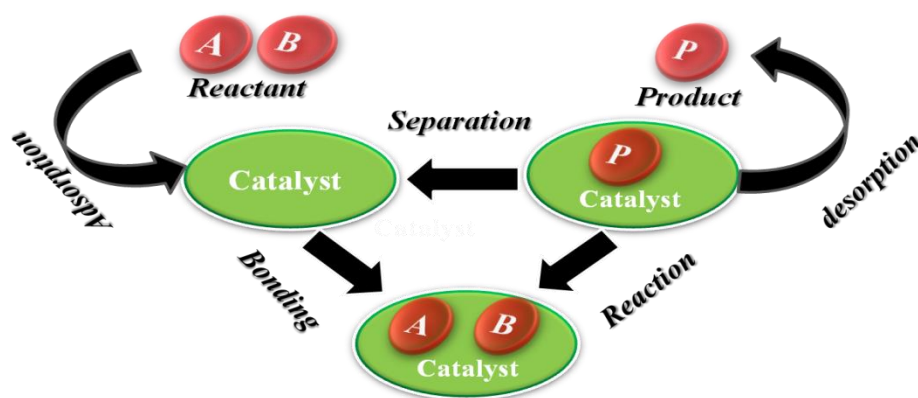
Catalysis plays an essential role in chemical reactions and it is heart of numerous chemical protocols, from academic research to industrial level.⁸ Catalysis has great importance because it affects our daily life. Main sectors of the world economy like energy production, polymer production, chemicals production, pollution control and food industry, involve catalytic processes. In pharmaceutical industries for drug production which save lives and cure many health problems, many a time catalysts are used for fast and better yield. Catalysis contribute the method by which chemical transformations take place that enabling the commercially sufficient formation of desired materials. By the use of catalysts we get more sustainable, green and cost-effective methods.⁹

There are two types of catalytic reactions: Heterogeneous and Homogeneous .When phase of catalyst and reactant used in reaction is same, such reactions are known as homogeneous catalytic reactions. Generally, in these reactions all the reactants/catalysts are either in liquid phase or gas phase. For most industrial processes, homogeneous catalyst used in liquid phase for most industrial processes.¹⁰

When reactant and catalyst used in reaction are in different phase then such reaction is known as heterogeneous catalytic reaction. It is believed that the whole outer surface of catalysts does not take part in catalytic reaction. Only certain sites on the surface take part in reaction which is known as active sites on the catalysts. Adsorbed reactant atoms or molecules interact with these sites. Catalytic activities depend upon number of active sites present on catalytic surface which is expressed in term as turnover frequency. Turnover frequency means the number of molecules reacting per active site per second at condition of the reaction.

In a heterogeneous catalytic reaction, reactant to product goes through the following steps:

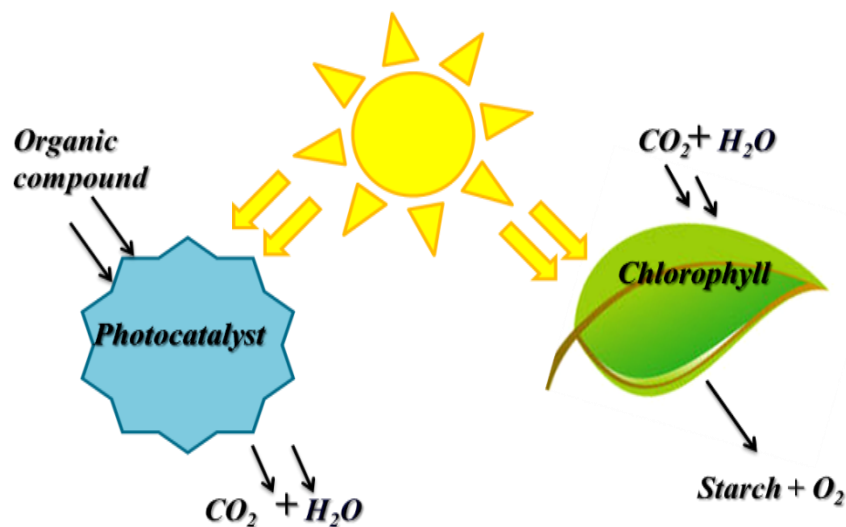
1. Transfer of reactant (R) from bulk fluid to catalytic surface
2. Reactant (R) diffusion to internal catalytic surface
3. Reactant (R) adsorbed on catalytic surface
4. Reactant (R) react on the catalytic surface to produce product
5. Product (P) desorbed from the surface of catalyst.



Scheme 1: Schematic representation of reaction process over the catalyst surface

Photocatalysis

The word “photocatalysis” came from Greek origin and composes of two words, the prefix “photo” means light and the word “catalysis” means is change the speed of the reaction.. Chlorophyll is one of natural occurring photocatalyst. The difference between chlorophyll to man-made photocatalyst is that chlorophyll absorbs sunlight to convert water and CO_2 to O_2 and glucose, but photocatalyst creates holes and electrons which break the large organic molecules to CO_2 and water in the presence of light and water as shown in scheme.2. Heterogeneous photocatalysis includes several reactions such as dehydrogenation, mild/total oxidation and transfer of hydrogen, removal of gaseous pollutant, water detoxification, deuterium-alkane isotopic exchange and degradation of organic pollutants. Heterogeneous photocatalysis is a technique, which is valuable for environmental and energy purposes. Heterogenous catalysts have many advantages because they are cheap, non-toxic, reusable and easy to separate from reaction mixture. Some common semiconductors used as photocatalysts are: TiO_2 , ZnO , CdS , WO_3 , SnO_2 , ZnS , CdTe , $\alpha\text{-Fe}_2\text{O}_3$, AgNbO_3 and SrTiO_3 .¹¹



Scheme 2: Photocatalysis process (Photosynthesis v/s Semiconductor)

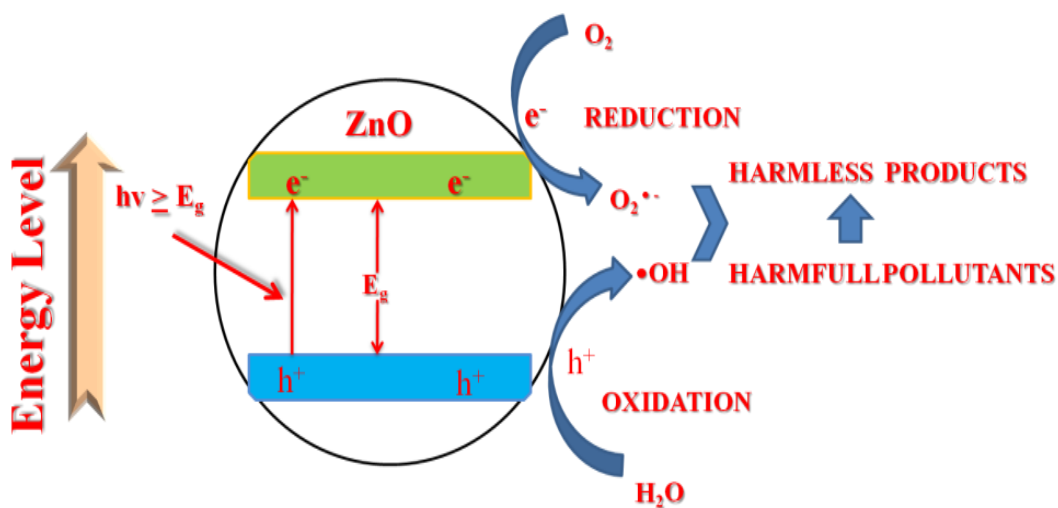
ZnO as Photocatalyst

Wurtzite phase of ZnO is mostly used as a photocatalysts. ZnO is believed to be more efficient than TiO_2 due to its high quantum yield in many cases.^{12,13} Nanostructures of ZnO semiconductor have large bandgap $E_g = 3.37$ eV, therefore they suffers from intrinsic limitation

which is responsible for only 4% absorption of the UV light of solar energy.¹⁴ ZnO is a II-V oxide semiconductor having excitation binding energy about 60 meV and bandgap of 3.37 eV.¹⁵ ZnO NP (nanoparticles) are widely used for electronic and optoelectronic applications which includes LEDs, field-emission devices, solar cells, ultra-violet laser diodes, photocatalysts, spintronic and also for piezoelectronic devices because of its good piezoelectric properties, optoelectronic properties, biocompatibility, thermal stability and environmentally friendly nature.^{16,17} There are many reports that describes progress in expansion and applications of various ZnO nanostructures. Rock-salt and zinc-blends are different structures of ZnO, but wurtzite structure being thermodynamically more stable.¹⁶

Mechanism of working of ZnO as a Photocatalyst

In photocatalytic processes, ZnO absorb radiations with energy ($h\nu$) greater than or equal to its original bandgap energy. Absorption of photons results in the excitation and electron transfer to the conduction band (CB) from valence band (VB) which leads the formation of holes in the valence band. These h^+ and e^- recombines and emits energy which resulting in low quantum yield of photocatalytic reactions. This recombination rate of holes and electrons depends on various parameter like shape, size and bandgap.^{17, 18} These holes and electrons at the catalytic surface of ZnO results in oxidation and reduction reactions to form superoxide anion radicals ($O_2^{\cdot-}$) and hydroxyl radicals ($\cdot OH$), respectively. These $\cdot OH$ radicals react with harmful pollutants to give harmless products as shown in Scheme.3.



Scheme 3: Photocatalysis at the surface of ZnO

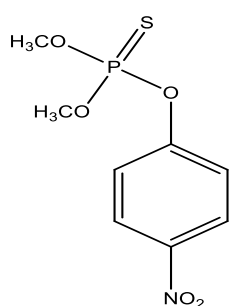
Modification strategies for better photocatalytic activity

Most of the widely used photocatalysts have wide energy gap, thus their activation energy is very high (UV irradiations), which make its use difficult on large scale and is less economical. Therefore, in these days, research is focused on photocatalysis by visible light as there is only 4% of UV irradiation in sunlight whereas nearly 45% of sunlight consist of visible light.¹⁴ On the way to make photocatalyst solar light active, plasma coupling, nonmetal and metal loading, self-loading of crystal and band matching with semiconductors have been described in literature.^{19, 20, 21} ZnO photocatalysts gives a poor activity under solar radiation. Metals and non-metals loading is widely applied to expand the range of wavelengths absorbed by ZnO by altering electronic band structure without decreasing photocatalytic activity in visible-light spectrum. Usually this is done by narrowing bandgap of ZnO, which happens through doping ZnO that may be result of i) introducing new localized energy level between the bandgap of ZnO, ii) lowering the conduction band and iii) the elevation of the valence band maximum.²² Doping of transition metal (TM) in ZnO crystal lattice is quite popular strategy for making ZnO active in visible-light.²³ Change in the environment of Zn in ZnO crystal structure and electronic band structure arise many crystal defects like oxygen vacancies by additions of TM cations. Oxygen vacancies are good electron traps that can increase efficiency of photo-generated electron-hole separation.²⁴ Due to the difference in stoichiometry and the existence of intrinsic defects like zinc interstitials (Zn_i), oxygen vacancies (V_O), and zinc vacancy (V_{Zn}), ZnO is intrinsically n-type semiconductor. Doping of metals in ZnO controls its structure and therefore magnetic, electrical and optical properties, which leads to the number of changes like transparency, bandgap, magneto-optical properties, ferromagnetism and piezoelectric properties.^{16, 17, 25} Copper (Cu) is a cheap element and its size is nearly same as Zn, hence copper cation can easily penetrate the substitutional sites of ZnO crystal lattice and modify absorption/emission spectrum of Zinc Oxide in solar light.²⁶

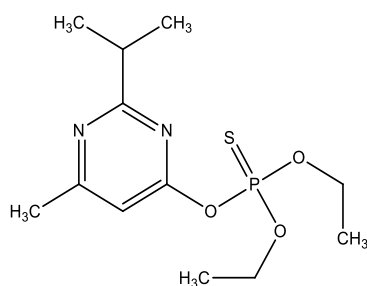
Pesticides

Pesticides are organic species which were used to increase the production of crops by killing unwanted pests. Pesticides, insecticides can easily diffuse into ground-water/ surface water which become a big problem in present days. The pesticides have longer half life time,

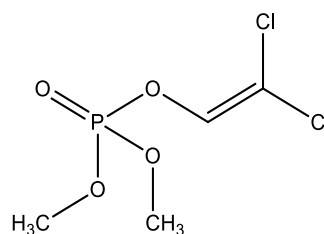
they don't degrade easily as they accumulate in eco-system and cause many health problems. The use of organophosphorus pesticides is increasing day by day and methyl parathion, dichlorvos, diazinon and fenthion are member of this family. They cause many health problems like abdominal pain, cough, skin irritation and decrease in size of red blood cells. It is reported that methyl parathion gets completely oxidized by Fenton system in UV light to produce sulphuric acid, oxalic acid and in other harmless products. Malwa region of Punjab, India is found to be highly contaminated by pesticides due to their overuse. Analysis of water and agriculture products from this region provides the proof for the presence of pesticides.



Methyl Parathion



Diazinon



Dichlorvos

Literature review

Synthesis, characterization and applications of nanomaterials have strongly promoted its broad use as catalysts. Nanomaterials have been the centre of scientific interest because of structures and high surface areas. These NP can be synthesized through various pathways and have various applications. Like ZnO can be obtained from metallurgical processes as well as from Chemical process. For metallurgical processes, ISO 9298 standard classifies ZnO in two types on the basis of processes they obtained: First is American process developed by Samuel Wetherill (also named as direct process) which includes reduction of zinc ore by heating coal then oxidation of Zn vapors. The particles obtained are usually of needle shaped and some are of spherical shape.²⁷ Second method is French method (indirect process) in which metallic zinc ore is vaporized at 910 °C in furnace, Zn vapors react with oxygen present in air to give ZnO. The ZnO particles obtained have size from 0.1 to few micrometers. This method is carried out in vertical furnace and ZnO obtained by this method is purer than American process.²⁸ There are many laboratory methods for the synthesis of ZnO nanoparticles from precursors like ZnCl₂, NaCl, Na₂CO₃ etc. Weiqin *et al.* prepared ZnO NP by using Na₂CO₃ and ZnCl₂ with mechano-chemical method to get ZnCO₃ by 6 h milling which was further calcined at 400-800 °C. Studies

showed that size of NP depends upon calcination temperature and the milling time for preparation of ZnCO₃. Size of NP was reduced by increasing milling time but increase in calcination temperature results in increase in the particle size.²⁹ Jianguo *et al.* decolorized the rhodamine B aqueous solution by ZnO hollow sphere prepared from different molar ratio between 0-20 of ZnCl₂ and glucose by hydrothermal method at 180 °C for 24 h then calcined at 500 °C for 4 h in air. The results showed that the size, specific surface area, thickness of shells and activity of NP depends on the molar ratio of Zinc chloride and glucose. The sample with high ratio showed better catalytic activity than P25-TiO₂ probably because hollow spheres showed unique hierarchical nonporous structure thus well-organized transfer of reactant to active sites which increase photocatalytic activity of ZnO particles.³⁰

Kansal *et al.* demonstrated photocatalytic degradation of lignin by using TiO₂ and ZnO in UV radiations at different pH (3 to 11) and different concentrations of oxidant (3.06×10^{-6} M to 15.3×10^{-6} M) and lignin (10–100 mg/L). Variations in amount of photocatalysts show no effect at all but rate of photodegradation was maximum at the pH 11 and for lower concentrations of lignin. Photodegradation rate increased in the presence of ZnO as it absorbs large portion of UV radiations than TiO₂.¹² Senthilnathan *et al.* degraded the commonly used pesticides like methyl parathion and diclorvuos with TiO₂. N-doped TiO₂ was used to degrade both the pesticides under UV and visible light. Nitrogen used for doping was immobilized obtained from different organic compound.³¹ Birben *et al.* demonstrated the humic acid photocatalytic degradation by Ce doped ZnO nanoparticles. Zn(NO₃)₂·6H₂O water solution at pH 10-11 was used to synthesize ZnO by hydrothermal method at 175 °C for 16 h and same procedure was repeated after adding 1% molar concentration of Ce.³²

Sini *et al.* studied the superior activity of Co doped ZnO nanodiscs and nanorods using Zinc chloride, hexamethylenetetramine and cobalt chloride as starting materials. In this facial wet method ZnO NP in 1:1 ratio of HMTA and Zn²⁺ water solution were stirred and heated for 20 hours at 80 °C and Co doped ZnO particle obtained by adding CoCl₂·6H₂O in ZnCl₂ HMTA solution by same procedure. Photocatalytic activity of ZnO and Co doped ZnO studied by degrading methyl blue in sunlight.³³

Ji *et al.* described a novel catalyst prepared by a modified polymerizable complex method. Water soluble tantalum obtained from tantalum oxide and potassium oxide, both were heated at 400 °C in K: Ta =1:10. For Ta doped ZnO, Zinc nitrite mixed with citric acid in DI (deionized)

water and stirred for 1 h then citric acid-tantalum in ethylene glycol added with zinc nitrite solution in the presence of nitric acid as a catalyst (1:100). Mixture was sonicated for 15-20 min and evaporated to 70 % of its original weight. 3.5×10^{-3} g/ml of HPC (hydroxypropyl cellulose) and 2.5×10^{-1} g/ml acetylacetone was added to the mixture as steric dispersant and stabilizer, then mixture was aged for 24 h at normal temperature in air after that baked at 140 °C for 12 h for poly-esterification at Ta²⁺ doping caused the number of change in ZnO lattice. 1 mol % of Ta²⁺ loading in ZnO nanocrystals showed excellent photocatalytic activity than ZnO nanocrystals.³⁴

Kanade *et al.* synthesized self-assembled aligned hexagonal prismatic Cu doped ZnO of average particle size in range of 40-85 nm. The Cu-Zn oxalates were prepared by using water or methanol or ethylene glycol as solvent. Zinc acetate, oxalic acid, CuCl₂ in any of these solvent and mixture was decomposed at 450 °C in aerobic conditions. Nanoparticles produced hydrogen from water, H₂S and organic waste.³⁵ Vignesh *et al.* used zinc sulfate (0.1 M) and NaHCO₃ (0.2 M) to synthesize ZnO nanoparticles. The NaHCO₃ solution was drop wise added to zinc sulfate solution under continues stirring and then obtained precipitates washed and calcined at 350 °C for 3 h. Zinc oxide with 10% of silver iodide gets suspension of ZnO, KI and AgNO₃ with ammonium hydroxide by vigorous stirring. The molar ratio of I⁻/Ag⁺ was 1:1. The photocatalytic decolorization of rosaniline hydrochloride dye (RA) was 1st order reactions and effect by factors like pH, catalyst concentration and concentration of RA. AgI sensitized ZnO showed best catalytic activity at pH 8 and concentration of catalyst 0.3 g/L.³⁶

Mohammed *et al.* prepared ZnO nanoparticles by colloidal solution of Zn(CH₃COO)₂·2H₂O and NaOH in ethanol then this colloidal solution was heated at 70 °C for 30 min after this NaOH was added to mixture and hydrolyzed at 60 °C for 2 h in commercial microwave. For 1 wt% of dopant manganese acetate mixed directly to zinc acetate during hydrolysis. Photocatalytic activity test by degradation of methylene blue. The high absorption of solar light proves the presence of defects in nanoparticles.³⁷ Shengwei *et al.* used zinc nitrite and PEG 2000 and urea solution in DI water in autoclaves and heated it at 180 °C for 12 h. This procedure gave the hierarchical flower like carbon doped ZnO super structure. The production of OH radicals detected with the help of photoluminescence technique and its photocatalytic activity was studied by degradation of dye Rh B.³⁸

Paul *et al.* discovered that ZnO at nanoscale have antimicrobial activity thus it can be used for food packaging. ZnO particles prepared by using ZnCl₂ and Na₂CO₃ as precursors, both of

them milled to get ZnCO_3 dust and then ZnCO_3 and NaCl were milled again at low temperature. These nanoparticles were used for food packaging because of their antimicrobial properties.³⁹

Mehdi *et al.* prepared the Cu doped ZnO NP for the degradation of Organophosphorus insecticide named as diazinon. CuCl_2 was drop wise added to the ZnCl_2 under constant stirring then pH of solution was maintained by adding ammonia. After 3 h stirring white precipitates were obtained and dried. Degradation of diazinon follows the pseudo 1st order kinetics. Cu-doped ZnO NP gave better efficiency than ZnO NP under UV irradiations.⁴⁰

Research gaps

The literature revealed that various dyes and other organic harmful compounds have been degraded using ZnO nanoparticles under UV light irradiation. However, there are some limitations for the use of ZnO as photocatalyst such as lack of visible light activity and slow degradation rate of intermediates which are sometimes more toxic than parent molecules. The improvement in photocatalytic activity of ZnO can be achieved by:

- (i) Alteration in the size and shape of ZnO that can improve the electronic properties.
- (ii) Metals loading of over different shapes of ZnO NPs can further give better catalytic activity.

Although, these modified ZnO NP exhibits higher photocatalytic activity than unmodified ZnO have been well considered for degradations of many environment pollutants like dyes and many other organic compounds. Yet it is rarely used of degradation for pesticides.

Objectives

- (i) To prepare various nanostructures of ZnO.
- (ii) To prepare Cu loaded ZnO composites by different methods.
- (iii) To study comparative catalytic activity and physiochemical properties of prepared nanocomposites for the degradation of methyl parathion.

Materials and Methods

Chemicals and reagents

Zinc nitrite hexahydrate ($\text{Zn}(\text{NO}_3)_2 \cdot 6\text{H}_2\text{O}$, 98%, Loba Chemie Ltd), Ammonia (NH_3 Merck Specialties Private Ltd), Zinc Chloride (ZnCl_2 , 97%, Loba Chemie Ltd), Sodium hydroxide (NaOH , 96%, Avantor Performance Material Private Ltd), Isopropyl alcohol, Argon gas, Polyvinyl Pyrrolidinone (PVP, 90%, Spectro Chem. Ltd), $\text{Zn}(\text{CH}_3\text{COO})_2 \cdot 2\text{H}_2\text{O}$, Cupric nitrite ($\text{Cu}(\text{NO}_3)_2 \cdot 3\text{H}_2\text{O}$, 99%, Loba Chemie Ltd).

Methods

Synthesis of ZnO Porous Spheres

Zinc nitrite hexahydrate, ammonia and starch were used for the preparation of porous ZnO as reported previously⁴¹. Starch (2.5 g) was dissolved in 150 mL of boiled deionized water (DI) to obtain clear starch solution. $\text{Zn}(\text{NO}_3)_2 \cdot 6\text{H}_2\text{O}$ (0.01 mol/L) was added to the clear starch solution followed by continuously stirring for 15 min at 80 °C. The pH of solution was maintained between 8-9 by slow addition of ammonia to get a milky solution. This solution was stirred further for 30 min at 85 °C. The resulted precipitates were centrifuged, washed with deionized water and ethanol, and dried at 50 °C. The dried powder was calcined at 500 °C in the presence of air to obtain ZnO spheres and were used for the further application.

Synthesis of ZnO flower like structures

In a typical procedure,⁴² 0.27 g of ZnCl_2 (2.0 mmol) and 0.27 g of NaOH (10.0 mmol) were dissolved in 30 mL of DI water and stirred for 5 min. The solution was transferred to Teflon lined stainless sealed autoclave and heated at 80 °C for 24 h, and the contents were cooled to the room temperature. The resulting white precipitates were separated by centrifuge, washed with distilled water and ethanol few times and dried at 60 °C for 12 h.

Synthesis of ZnO rod like structure

In typical procedure,⁴³ 1.68 g of PVP was dissolved in 80 ml of DI water and added 2.3 mmol of zinc acetate dihydrate along with stirring for 15 minutes followed by addition of 0.025 mol (1 g) of NaOH . The resultant solution was transferred to 100 mL of Teflon lined stainless steel autoclave. The autoclave was placed in furnace at 80 °C for 48 h and then cooled to room

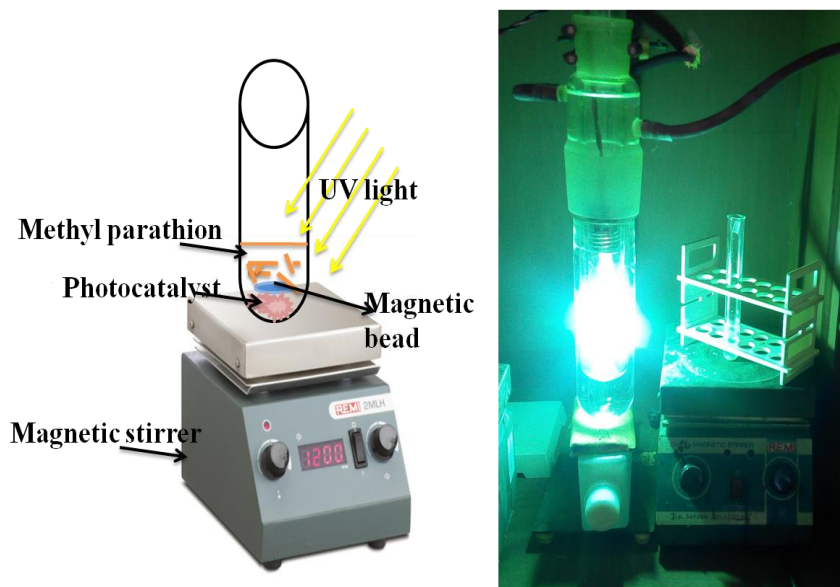
temperature. The resultant white precipitates were filtered and washed with DI water, with ethanol for few time and dried at 60 °C in air.

Photodeposition of metal ions such as copper ZnO NP

Cupric nitrite (Cu^{2+}) solutions (1wt%) were prepared and 1.574 mL of it was added in respective test tubes containing 100 mg of ZnO NP. Isopropyl alcohol and distilled water (1:1 mixture) was added in test tube. High purity argon gas was purged all the time to maintain anoxic conditions during the preparation of metal deposited ZnO. After that the test tubes were sealed with paraffin film. The contents in test tube were irradiated for 6 to 7 h in UV photo reactor. The obtained material was separated by centrifugation and washed with DI water and ethanol and dried the precipitates at room temperature.

Catalytic Activity

Catalytic activity and stability of prepared ZnO NP and Cu loaded ZnO NP catalysts was evaluated for the degradation of Methyl parathion by adding 20 mg of the catalyst to a solution of substrate (5 ml, 500 ppm) under constant stirring in UV radiation. The analysis of the products was done on UV spectrometer after a fixed time interval.



Scheme and image of Photocatalytic activity

Catalyst characterization

Different characterization techniques like SEM, Powder XRD, Solid-state UV absorption Spectroscopy, Zeta potential etc.

Ultraviolet-Visible Spectrophotometer (UV-Vis spectrophotometer)

The measurement of the reduction of a beam of light after it passes through a sample was done by UV-Vis absorption spectroscopy. Absorption spectra give the information about size distribution and nanoparticles formation. The principle of this instrument is that when sample is exposed to light (having suitable energy for electronic transition within the molecule), required energy is absorbed and the transition of electron takes place from lower energy level to higher energy level. Analytic Jena, SPECORD 205 instrument was used in this research in order to examine the characteristic absorbance band of the synthesized NPs. Aqueous suspension of all samples was analyzed in a 3.5 ml quartz cuvette in the detection range of 190-1100 nm.

Zeta Potential Measurement

When the NPs are suspended in an aqueous medium, the adsorption or ionization of ions takes place on the NPs surface, which leads to the formation of an electrical double layer resulting in the development of net charge, called zeta potential (ζ). Therefore, zeta potential is an important tool for understanding the state of NP surface and also predicts the long-term stability of the NPs. The measurements were carried out by means of Brookhaven Zeta Plus at 25 °C using a cuvette comprising a palladium electrode mounted on a machine support immersed in \approx 2-2.5 mL of NCs solution.

Scanning Electron Microscope (SEM)

The external morphology (shape and size) of the samples were analyzed by scanning electron microscopy. Morphology, topography, crystallographic and composition information about the sample surface can be investigated from SEM images. A beam of electrons is focused on a selected area of a sample at the time of SEM analysis and therefore an exchange of energy from the electron beam to the sample surface takes place. The electron gun produces electron at the top, referred to as primary electrons and these electrons are then analyzed, amplified and translated into images. JSM-7600F (0.1 to 30 kV) instrument was used for SEM images analysis,

where samples were placed on a specimen stub with conducting tape and then coated with a thin layer of gold to reduce sample charging.

Powder X-Ray Diffraction (P-XRD)

This technique is primarily used for identification of phase, composition and crystal system of the materials; it can also give information on unit cell dimensions. For the identification of crystal system, phase, composition and crystallinity of the materials this technique was used. PAN alytica X' pert PRO X-ray diffractometer with Cu K α ($\lambda = 1.54 \text{ \AA}$) radiation was used for XRD pattern analysis. A smooth plain surface paper was used to press the powder samples into a sample holder. The XRD study was done from Sophisticated Analysis Instrumentation Laboratory (SAI Lab), Thapar University, Patiala, India.

GC Chromatograph (GC)

This study was used to evaluate CO₂ released during the degradation of pesticides. It is done by injecting 1 mL of gaseous mixture from the test tube (tightly sealed) into GC (NUCON-5765) equipped thermal conductivity detector and Porapak-Q column having flow of nitrogen gas as carrier gas.

Results and Discussion

Solid- state UV-visible absorption

The solid-state UV-visible absorption spectra of ZnO nanoparticles (nanorods, nanoflowers and Nanospheres) as shown in Fig.1, showed strong absorption edges near about 397 nm, 390 nm and 400 nm respectively. The difference in absorption edges is mainly due to variation in the morphologies. Upon loading of Cu ions over ZnO, the absorption band edge shifted towards the higher wavelength i.e. red shift. This red shift could be attributed to strong interactions between the surface of ZnO and Cu.⁴⁴

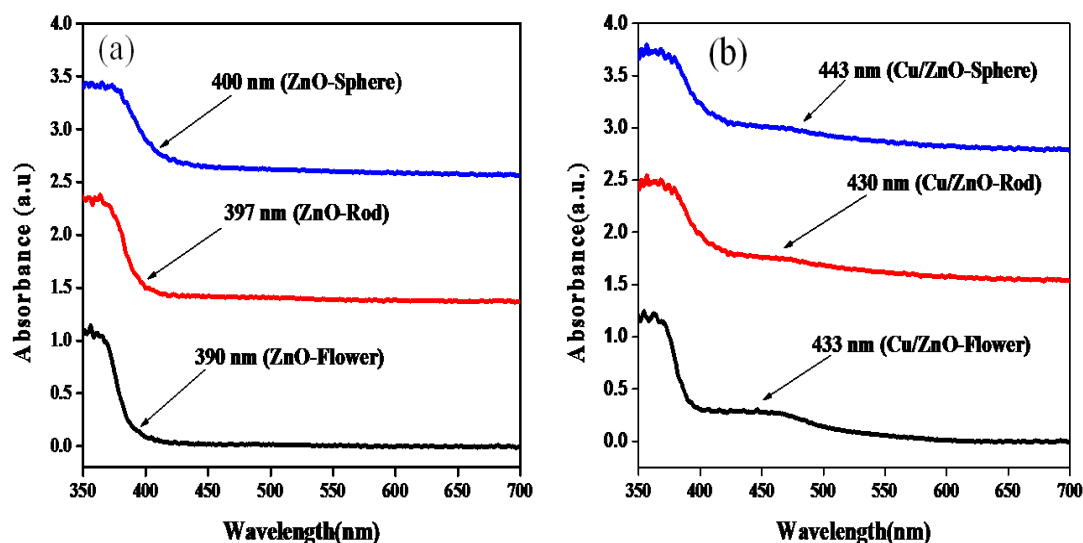


Fig.1 Solid state UV-Vis absorbance spectra of ZnO and Cu loaded ZnO nanoparticles

Zeta Potential

It is an indicator for the stability of colloidal suspension and electrostatic repulsion between similar and adjacent charge revealed by its magnitude. The surface charge of ZnO NP is +1.6 eV and Cu loaded ZnO NP is -0.313 eV.

X-Ray Diffraction

The phase and purity of as-prepared ZnO catalysts were analysed by X-Ray diffraction spectra (Fig.2). The narrow and sharp peaks in XRD show the crystalline nature of as prepared sample. The main diffraction peaks were found at 2 theta positions 31.98°, 34.33°, 36.48°, 47.57°, 56°, 62.9°, 66.1°, 68.28°, 72.81° and 76.97° with their corresponding planes (100), (002), (101), (102), (110), (103), (200), (112), (201) and (004) respectively. XRD peaks confirms the hexagonal crystal system with lattice parameters $a = 3.251 \text{ \AA}$, $b = 3.025 \text{ \AA}$ and $c = 5.201 \text{ \AA}$. An

increase in the intensity in XRD peaks was observed after Cu loading. It is noted that the no peak of copper oxide was found in XRD spectra and also that there was no influence of Cu-ions loading towards the phase and structure of ZnO crystal system. The crystallite size of ZnO nanoparticles was found to be 37.23 nm (nanospheres), 40.027 nm (nanorods) and 35.46 nm (nanoflowers). The Cu-loaded ZnO nanoparticles showed crystallite size 36.7 nm (spheres), 31.173 nm (nanorods) and 33.84 nm (nanoflowers). The crystallite size was reduced after Cu ions loading due to the formation of Zn-O-Cu complex at the surface, which hinders the growth of grains.⁴⁴ The diffraction peaks were indexed with the standard JCPDS card 00-001-0664 for ZnO nanoparticles and JCPDS card 01-079-2205 for Cu loaded ZnO nanocomposites

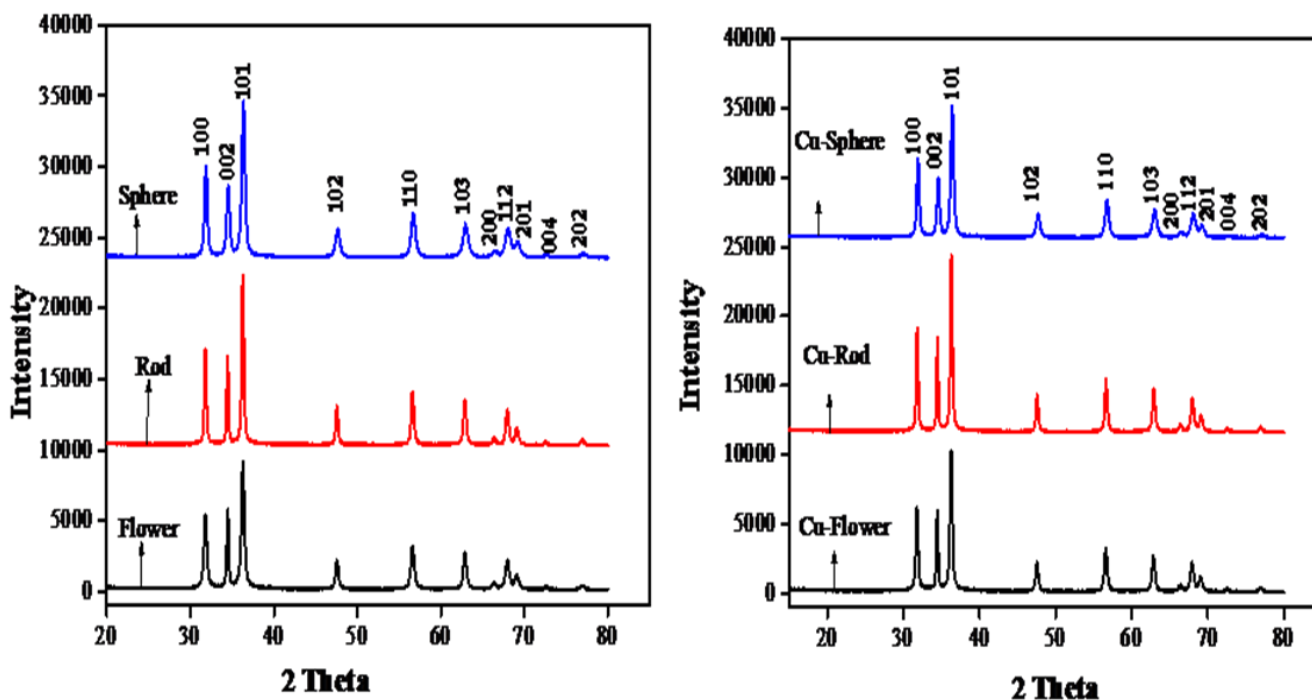


Fig. 2 X-ray diffraction pattern of ZnO nanoparticles and Cu loaded ZnO nanoparticles.

SEM and EDS

The various morphologies of ZnO NP have been studied by SEM images. The formation of NF (nanoflowers like structures), NR (nanorods like structures) and NS (nanospheres like structures) of ZnO, confirmed by SEM images are shown in Fig.3 (a and b), Fig.3 (c and d) and Fig.4 (e and f) respectively. The percentage and composition of loaded metal ions over as-synthesized various shapes of ZnO and Cu loaded ZnO nanorods was further confirmed by EDS analysis in Fig.4. and Fig.5. respectively

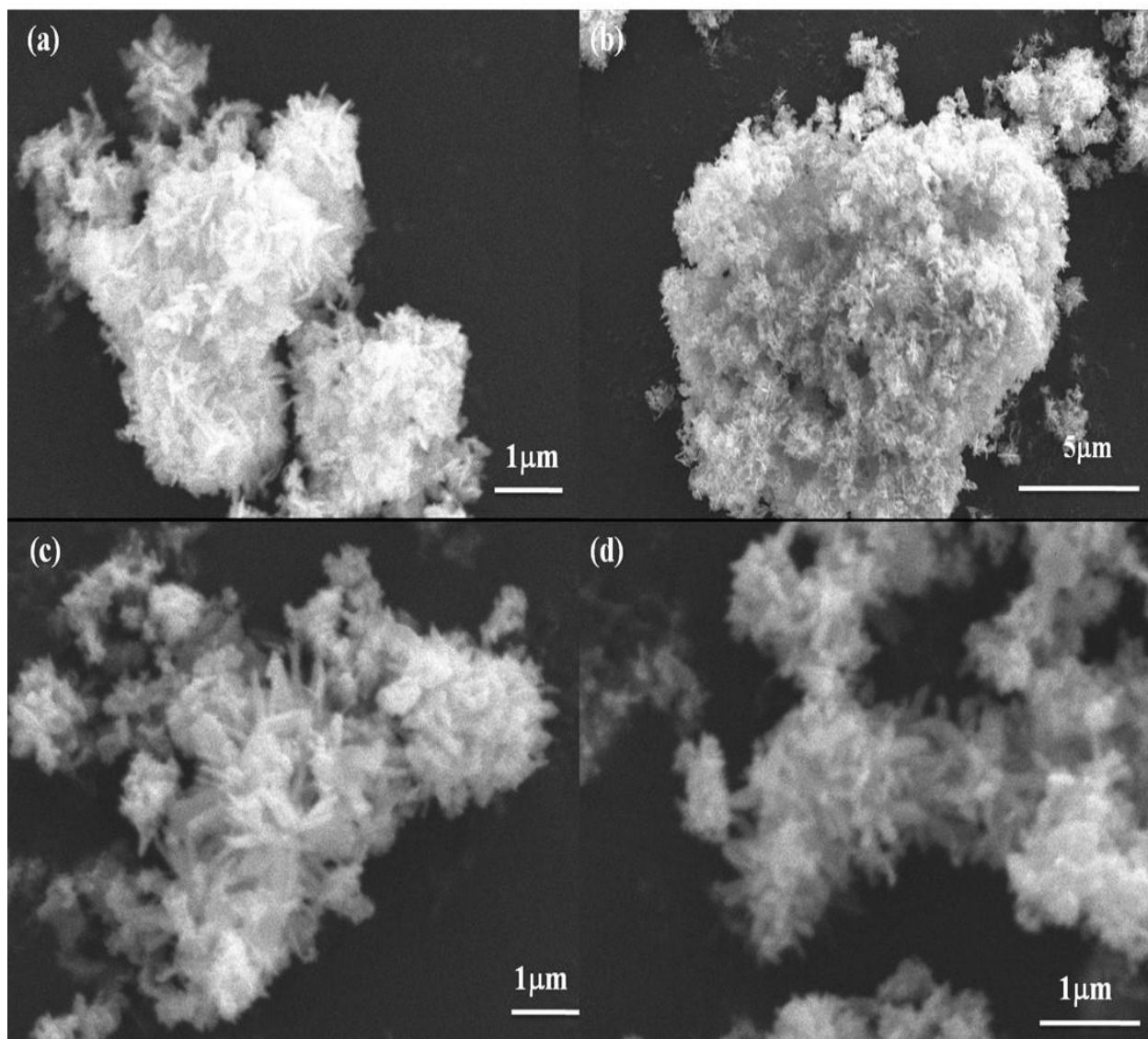


Fig.3. SEM images of ZnO (a and b) Nanoflower like, (c and d) Nanorods like.

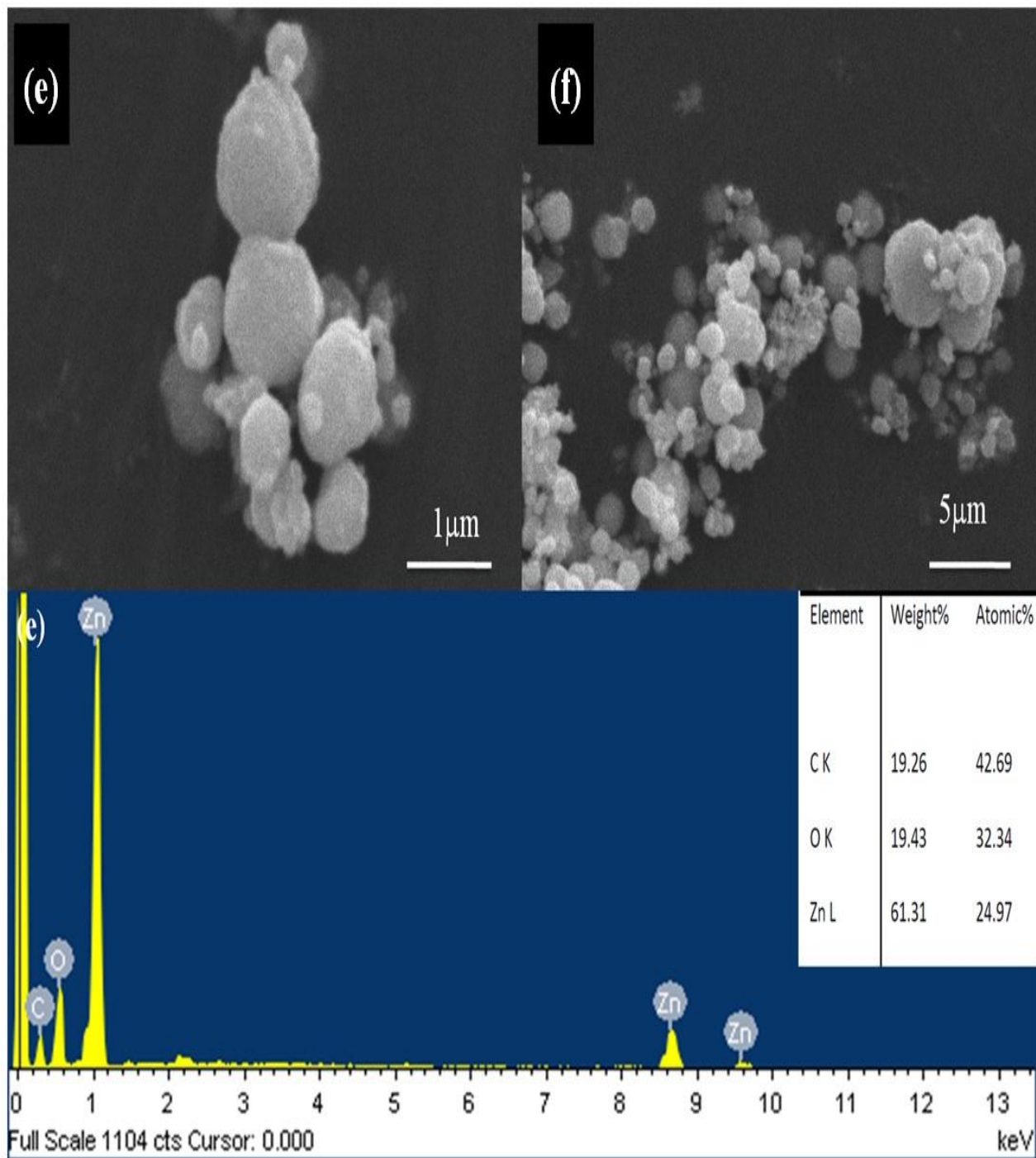


Fig.4. SEM images of (e and f) Nanospheres and EDS spectra

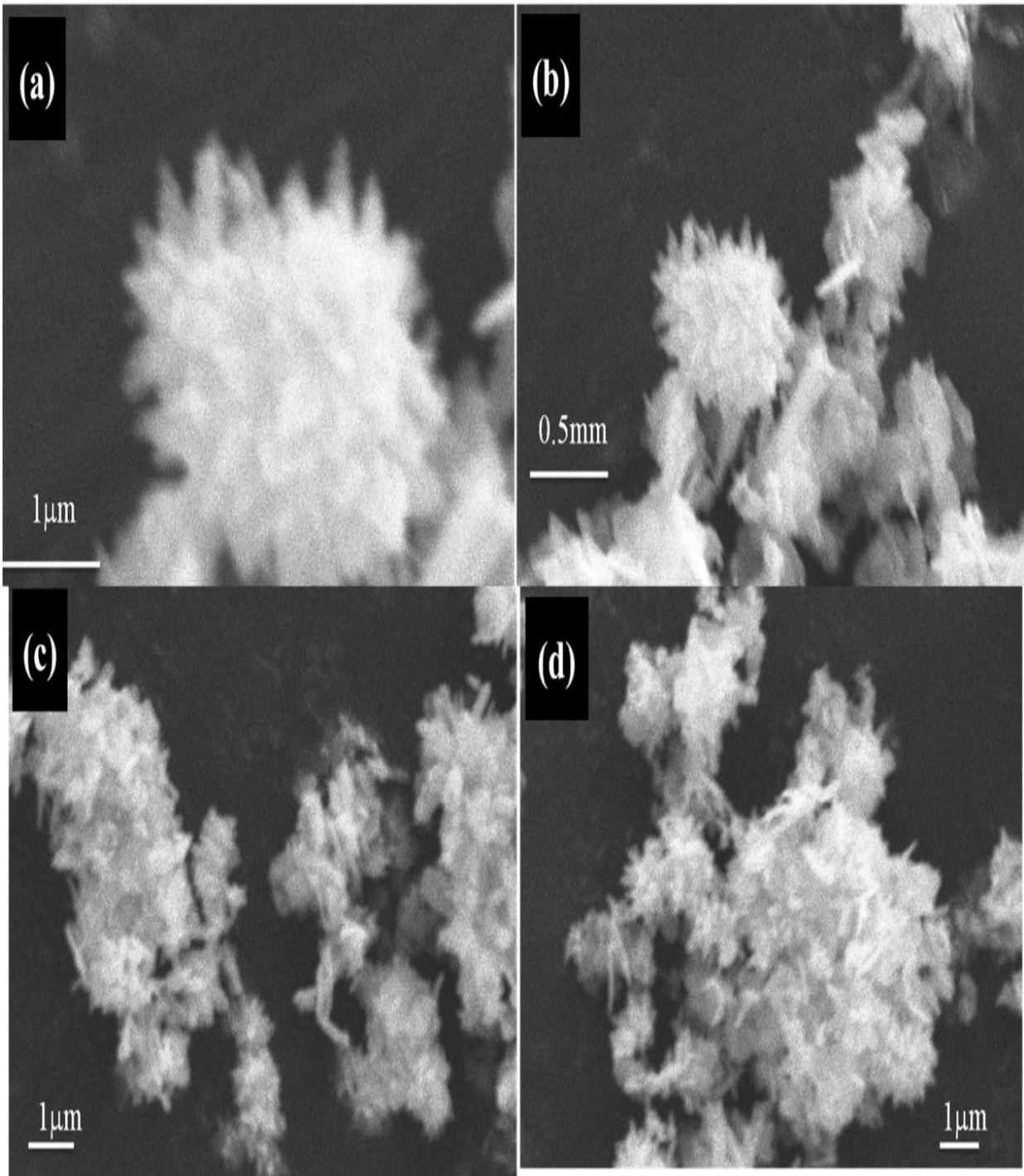


Figure.5. SEM images of Cu-ZnO (a and b) Nanoflower like, (c and d) Nanorods like.

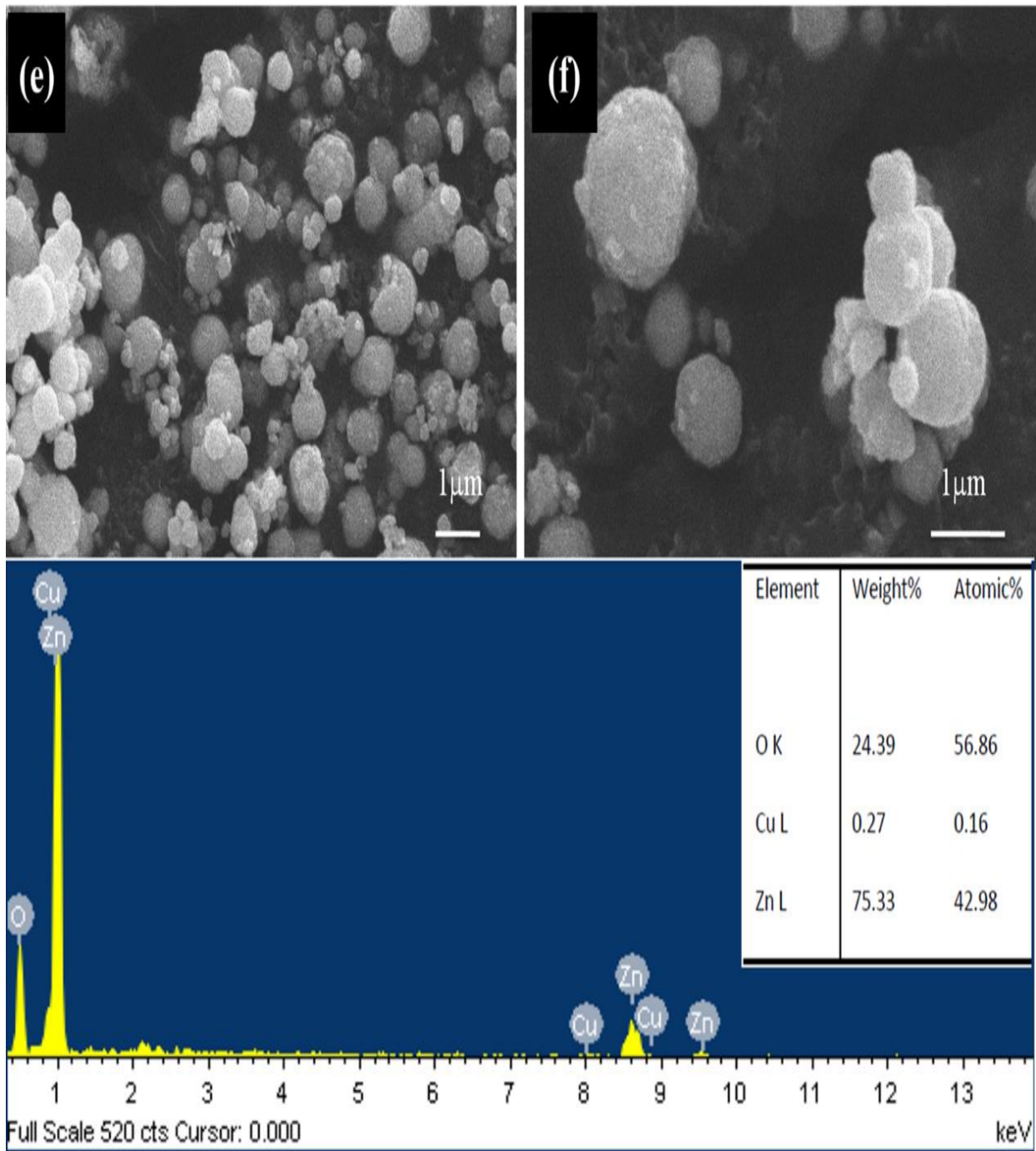


Fig.6. SEM image of (e and f) nanospheres like and EDS spectra

Photocatalytic activity

The catalytic performance of as-prepared nanocomposites of ZnO and copper loaded ZnO were evaluated for the degradation of methyl parathion pesticide. UV absorbance spectra of degradation of methyl parathion with ZnO NF, ZnO NR and ZnO NS are shown in Fig.7. The conversion and selectivity of obtained products were found to be greatly influenced by the synthetic method that indirectly control the size and with the loading of metal ion. ZnO NR took 3 h for catalytic degradation with 98% conversion while ZnO NF and ZnO NS took nearly 4 h and 6 h respectively for the degradation of pesticide (Fig.7). ZnO NR, ZnO NF and ZnO NS degraded 98%, 91%, and 65% of methyl parathion respectively under 3 h UV-light irradiation. ZnO NR showed more catalytic activity than ZnO NF and ZnO NS.

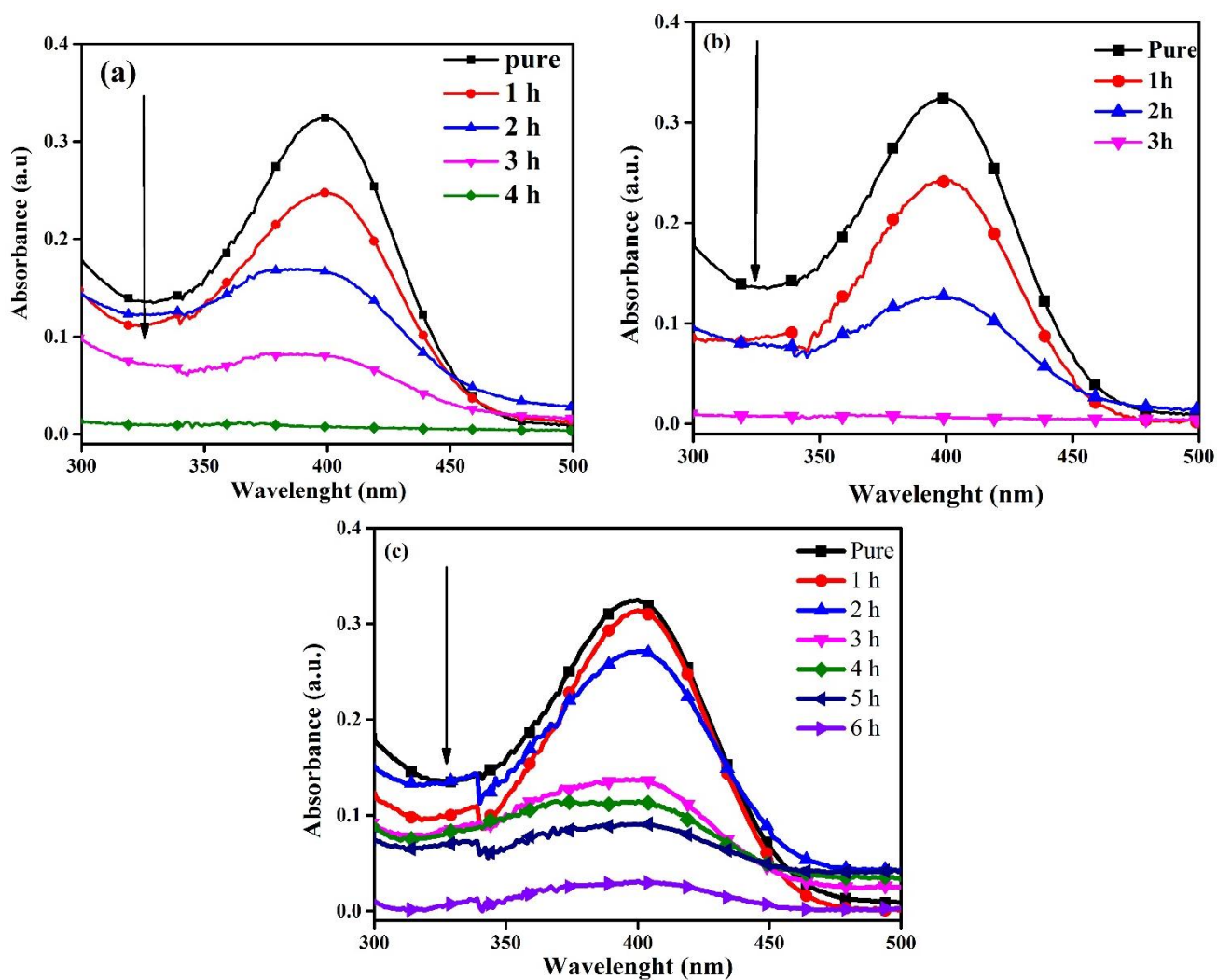


Fig.7. UV absorbance spectra of degradation of methyl parathion with (a) ZnO NF (b) ZnO NR (c) ZnO NS.

This may be because NR morphology offers smaller crystallite size which may provide more active sites for photocatalytic reaction and 1D ZnO NR has better charge transport through a one-dimensional direction, which decreases the rate of charge recombination and promotes the photocatalytic efficiency.⁴⁵

After metal loading recombination rate of photogenerated charge carriers at the surface of ZnO decrease. Solid UV absorbance shows the red shift in spectra with loading of Cu ion. Loading of Cu ion decrease the rate of recombination of charges which provide better activity.⁴⁵

⁴⁶ As shown in Fig.8. Cu loaded ZnO NR took 80 mins for 99% degradation of methyl parathion and Cu loaded NS took 120 mins and ZnO NS took nearly 280 mins for the degradation.

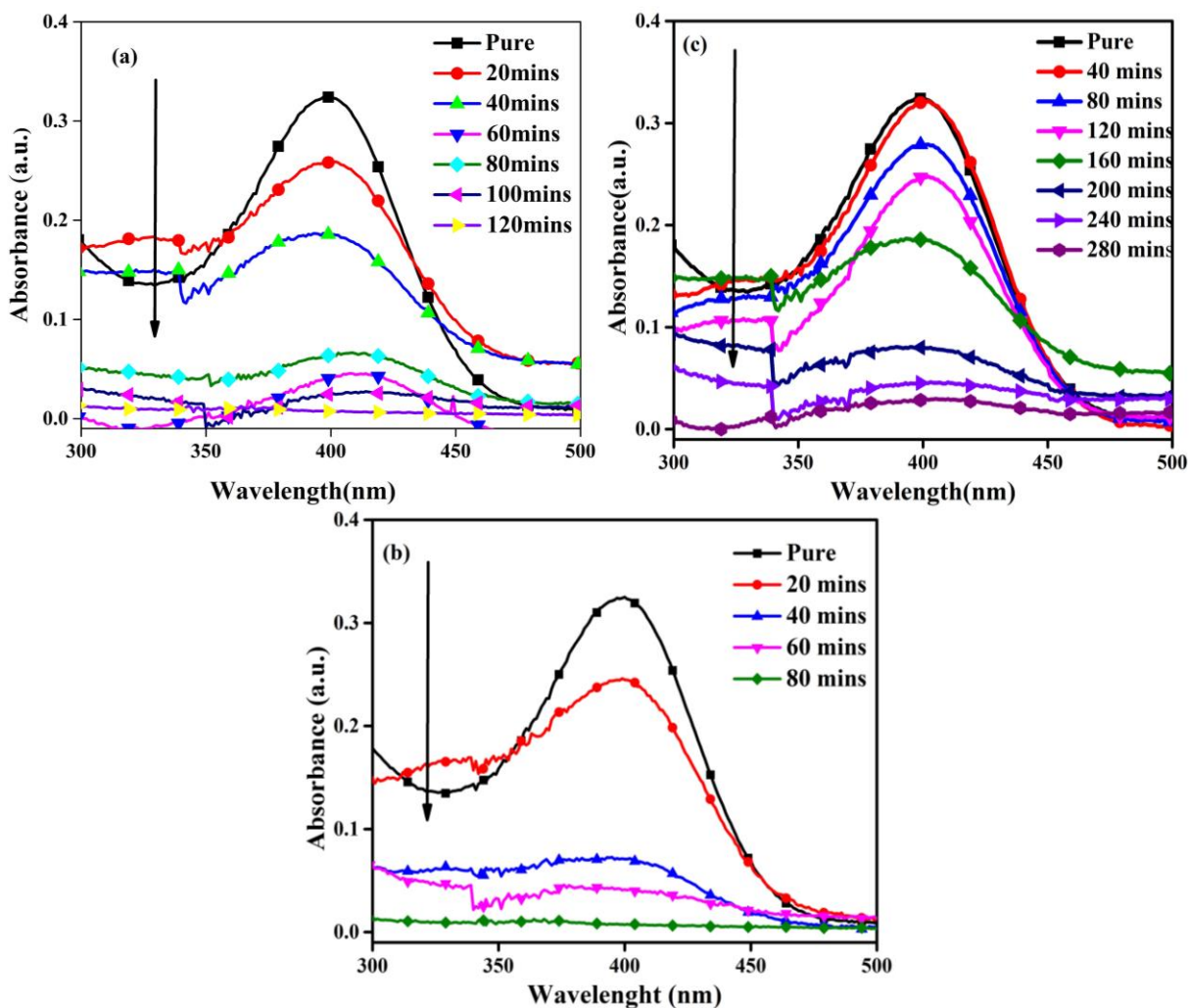


Fig.8. UV absorbance spectra of degradation of methyl parathion with (a) Cu-ZnO NF, (b) Cu-ZnO NR, (c) Cu-ZnO Ns.

The ZnO NR, ZnO NF and ZnO NS degrade 98%, 91% and 65% of pesticide in 3 h respectively whereas the Cu-ZnO NR, Cu-ZnO NF and Cu-ZnO NS degraded 99%, 86% and 14% of pesticide as shown in Fig.9. in 80 min respectively. The photodegradation efficiency of different nanocomposites calculated by following equation:

$$\eta \% = \left(1 - \frac{C}{C_0}\right) * 100$$

Where C=Final concentration, C₀=Initial concentration

Time versus Concentration graph shows that the reaction of Time versus Concentration graph shows that the reaction follows pseudo 1st order kinetics⁴⁰ shown in Fig.10

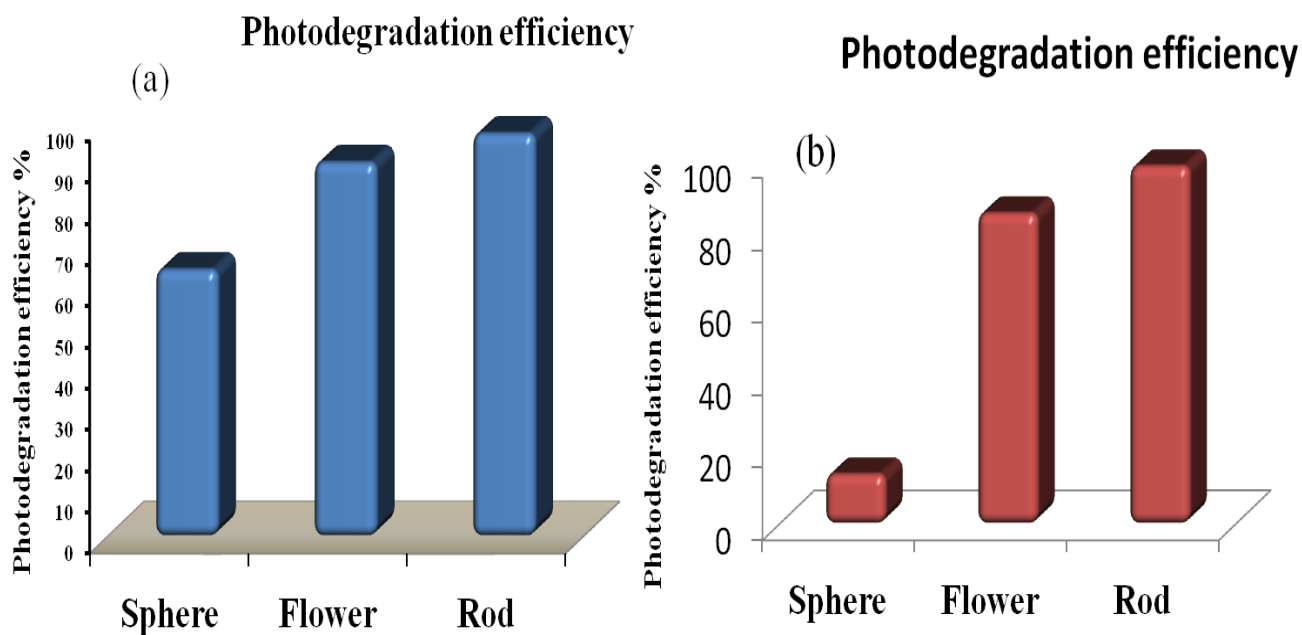


**Fig.9. Photodegradation efficiency $\eta\%$ with (a) ZnO NP in 4h
(b) Cu loaded ZnO NP in 80 min**

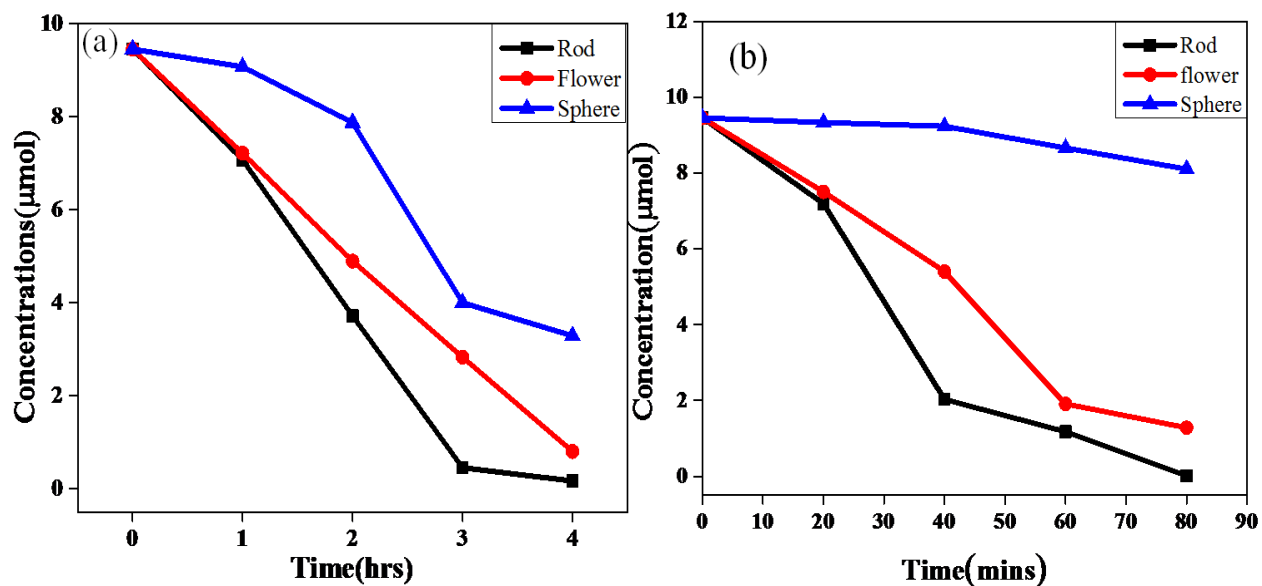


Fig.10. Time versus concentration graph of photodegradation (a) ZnO NP in 4 h (b) Cu loaded ZnO in 80min.

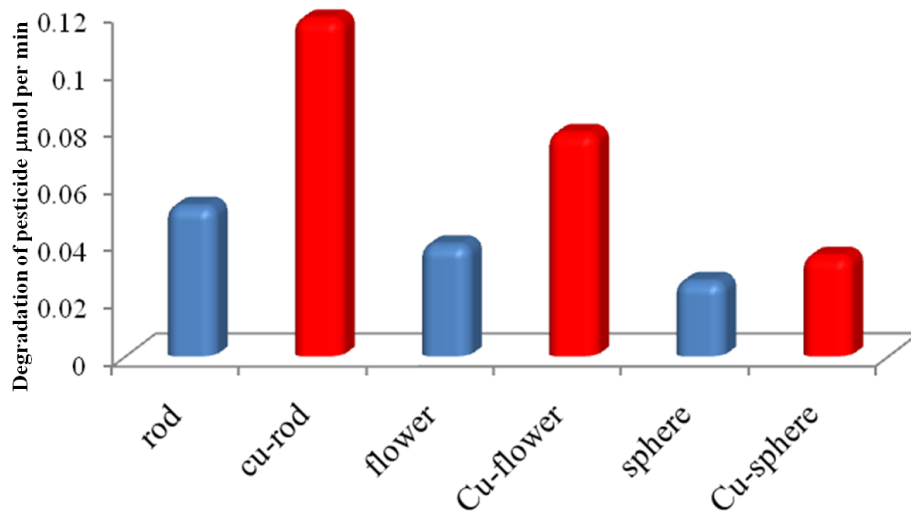


Fig.11. Comparative photodegradation of methyl parathion with different ZnO and Cu loaded ZnO NP

With the Cu loading the rate of degradation of methyl parathion increase because the rate of recombination of electrons/holes decrease.

Quantitative measurement of produced CO₂ by GC

The GC was used for the quantification of produced CO₂ during photodegradation of the pesticide. It was carried out by injecting 1 mL of gaseous mixture from the test tube (tightly sealed) into GC (NUCON-13A) equipped with thermal conductivity detector (TCD) and Porapak-Q column with nitrogen as a carrier gas. The oven temperature was set at 50 °C, injector and detector temperatures were set at 80 °C and 90 °C respectively. The quantification of CO₂ was done with standard 180 ppm as compared to retention time. The pesticide photooxidized to give smaller fragments that further degrade into smaller fragments like CO₂ and water. More photoactive catalyst produces more CO₂ which means comparatively more oxidation of the pesticide. The Cu loaded ZnO NR produced maximum amount of CO₂, showing it to be better photocatalytic active.

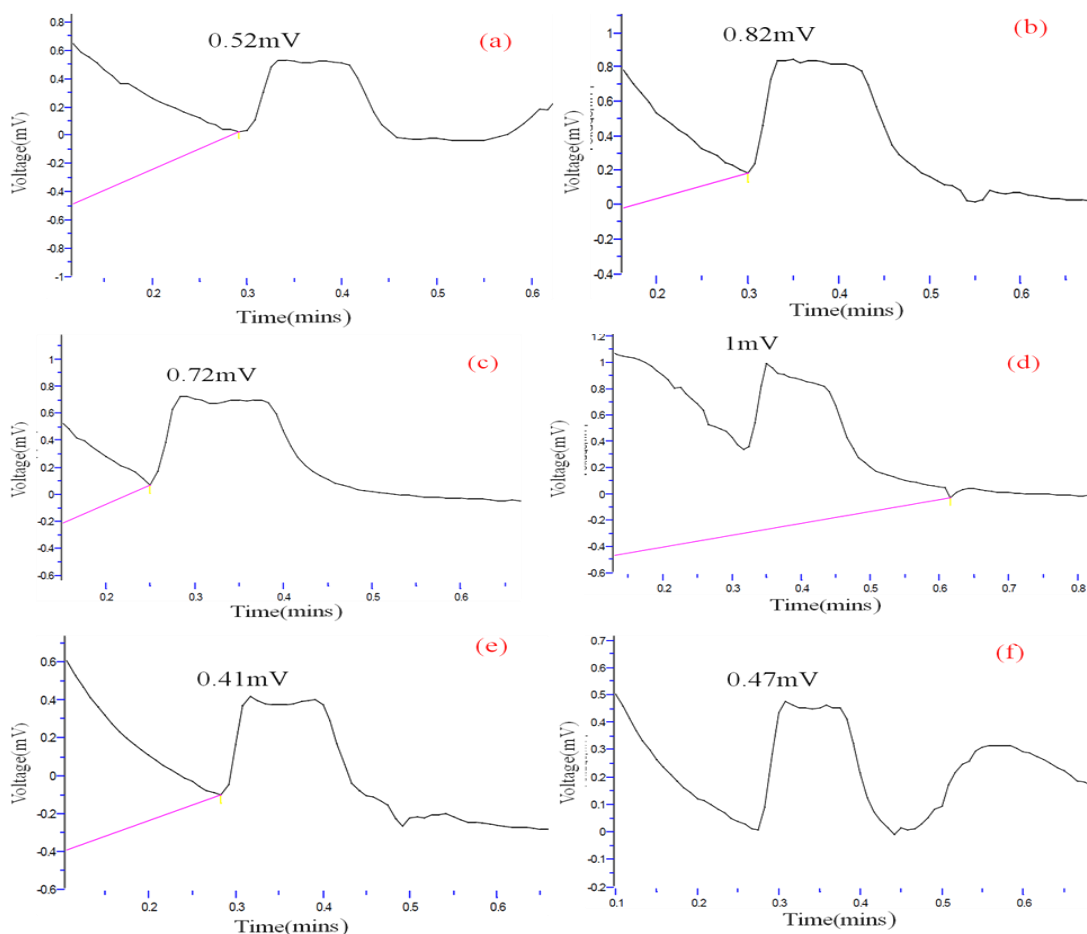


Fig.12. Quantification by GC graph using (a) ZnO NF, (b) Cu-ZnO NF, (c) ZnO NR, (d) Cu-ZnO NR, (e) ZnO NS, (f) Cu-ZnO NR as catalysts

The extent of photodegradation of pesticide was found by means of the amount of released CO₂ during the process. More the amount of released CO₂ means pesticide degrades properly into CO₂ and water. Lesser amount of produced CO₂ means other intermediate species were present during degradation which are not completely converted into CO₂. The CO₂ produced during the reaction by different morphologies of ZnO shown in Fig.12.

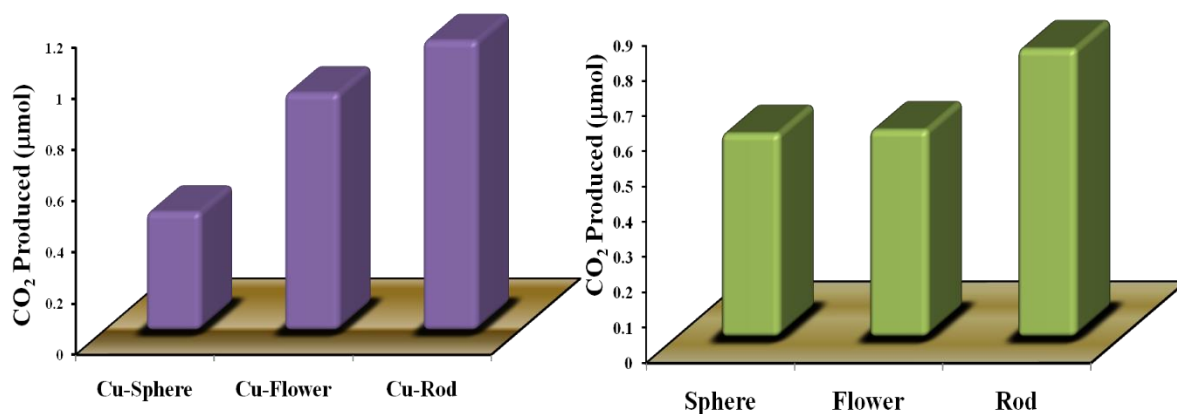


Fig.13. Amount of CO₂ produced by (a) ZnO NP, (b) Cu loaded ZnO NP

Reaction Mechanism

In photocatalytic processes, ZnO absorb radiations energy ($h\nu$) greater than or equal to its original bandgap energy. Absorption of photon results into electronic excitation and transfer of electrons to the conduction band (CB) from the valence band (VB) which forms holes in the valence band (migration of e^-/h^+ pairs). These holes and electrons at the catalytic surface of ZnO that results in oxidation and reductions reactions to form superoxide anion radicals ($O_2^{\cdot-}$) and hydroxyl radicals ($\cdot OH$), respectively. The $\cdot OH$ radicals react with methyl parathion and finally oxidize it into carbon dioxide. With the Cu loaded ZnO, the electrons form the conduction band of ZnO to conduction band to Cu metal thus the recombination of charge is decreased, therefore it gives better activity than bare ZnO. The photocatalytic reaction may be formations of reactive radical species through the following reactions.⁴⁶





(g)

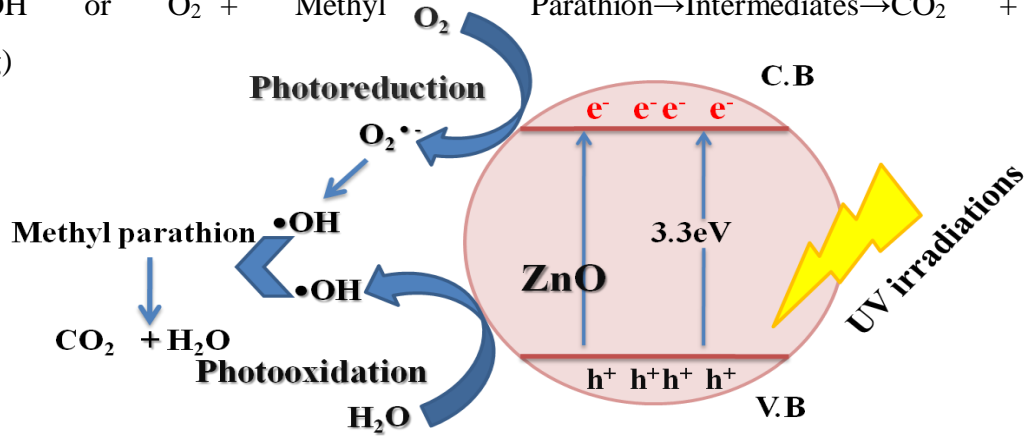


Fig.14. Photodegradation of methyl parathion with ZnO NP

Cu loading on ZnO lead to formation more holes, V_o and surface defects which increase the photocatalytic activity of the catalyst and the formation $\cdot\text{OH}$ radical for the photodegradation as per following reactions:

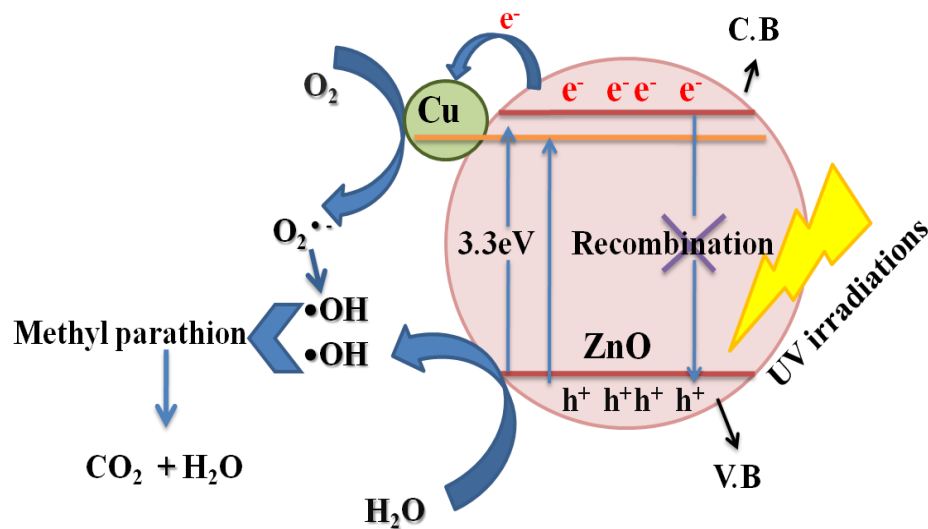
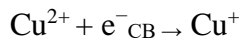


Fig.15. Photodegradation of methyl parathion with Cu loaded ZnO NP

Conclusion

In summary, various shape and size of ZnO nanoparticles have been synthesized and successfully applied for the photodegradation of methyl parathion. It was found that among the as synthesized various shapes, ZnO nanorods exhibited higher photodegradation efficiency. Furthermore, various morphologies of ZnO were decorated with Cu metal. As prepared ZnO nanorods showed almost complete conversion (~ 98%) of methyl parathion to CO₂ and water molecules in 3 h under UV light irradiation. However, Cu loading over ZnO increases the photodegradation efficiency (~99% 1) in 80 min. This increase in the conversion efficiency and rate of photodegradation could be attributed to the less rate of recombination due to Cu loading, narrow bandgap and anisotropic morphology.

Reference

1. Chorkendorff, I.; Niemantsverdriet, J. W., Concepts of modern catalysis and kinetics. *John Wiley & Sons*. **2006**
2. Laidler, K. J.; Cornish-Bowden, A., Elizabeth fulhame and the discovery of catalysis: 100 years before Buchner. *Cornish-Bowden*. **1997**, 123-126.
3. Yan, K.; Lafleur, T.; Liao, J., Facile synthesis of palladium nanoparticles supported on multi-walled carbon nanotube for efficient hydrogenation of biomass-derived levulinic acid. *J Nanopart Res*. **2013**, *15*, 1906.
4. Qiao, Y.; Li, H.; Hua, L.; Orzechowski, L.; Yan, K.; Feng, B.; Pan, Z.; Theyssen, N.; Leitner, W.; Hou, Z., Peroxometalates immobilized on magnetically recoverable catalysts for epoxidation. *ChemPlusChem*. **2012**, *77*, 1128–1138.
5. Yan, K.; Jarvis, C.; Lafleur, T.; Qiao, Y.; Xie, X., Novel synthesis of Pd nanoparticles for hydrogenation of biomass-derived platform chemicals showing enhanced catalytic performance. *RSC Adv*. **2013**, *3*, 25865-25871.
6. Cao, Z.; Jiang, H.; Luo, H.; Baumann, S.; Meulenberg, W. A.; Voss, H.; Caro, J., Simultaneous overcome of the equilibrium limitations in BSCF oxygen-permeable membrane reactors: Water splitting and methane coupling. *Catal. Today*. **2012**, *193*, 2–7.
7. Yan, K.; Lafleur, T.; Wu, G.; Liao, J.; Ceng, V.; Xie, X., Highly selective production of value-added γ -valerolactone from biomass derived levulinic acid using the robust Pd nanoparticles. *Appl. Catal.* **2013**, *468*, 52-28.
8. Hemalatha, K.; Madhumitha, G.; Kajbafvala, A.; Anupama, N.; Sompalle, R.; Roopan, S. M., Function of nanocatalyst in chemistry of organic compounds revolution: An overview. *J. Nanomaterials*. **2013**, Article ID 341015.
9. Polshettiwar, V.; Varma, R.S., Green chemistry by nanocatalysis. *Green Chem*. **2010**, *12*, 743–754.
10. Fox, M. A.; Dulay, M. T., Heterogeneous photocatalysis. *Chem. Rev*. **1993**. *93*, 341-357.
11. Hernandez-Ramirez, A.; Medina-Ramirez, I., Photocatalytic Semiconductors: Synthesis, Characterization and Environmental Applications. *Springer*. **2014**.
12. Kanasl, S.; Singh, M.; Sud, D., Studies on TiO₂/ZnO photocatalysed degradation of lignin. *J. Hazard. Mater*. **2008**, *153*, 412–417.

13. Tain, C.; Zhang, Q.; Wu, A.; Jaing, M.; Liang, Z.; Jiang, B.; Fu, H., Cost-effective large scale synthesis of ZnO photocatalyst with excellent performance for dye photodegradation. *Chem. Commun.* **2012**, *48*, 2858–2860.
14. Wang, Z.; Liu, Y.; Huang, B.; Dai, Y.; Lou, Z.; Wan, G.; Zhang, X.; Qin, X., Progress on extending the light absorption spectra of photocatalyst. *Phys. Chem. Chem. phys.* **2014**, *16*, 2758-2774
15. Jagadish, C.; Pearton, S. J., Zinc Oxide Bulk, Thin Films and Nanostructures: Processing, Properties, and Applications. *Elsevier*. **2011**.
16. Morkoc, H.; Ozgur, U., Zinc Oxide: Fundamentals, Materials and Device Technology, *John Wiley & Son*. **2008**
17. Klingshirn, C. F.; Waag, A.; Hoffmann, A.; Geurts, J., Zinc Oxide: From Fundamental properties towards novel applications. *Springer*. **2010**.
18. McLaren, A.; Valdes-Solis, T.; Li, G.; Tsang, S. C., Shape and size effects of ZnO nanocrystals on photocatalytic activity. *J. Am. Chem. Soc.* **2009**, *131*, 12540–12541.
19. Dong, S.; Feng, J.; Fan, M.; Pi, Y.; Hu, L.; Han, X.; Liu, M.; Sun, J.; Sun, J., Recent developments in heterogeneous photocatalytic water treatment using visible light-responsive photocatalysts: a review, *RSC Adv.* **2015**, *5*, 14610–14630.
20. Wang, Y.; Wang, Q.; Zhan, X.; Wang, F.; Safdar, M.; He, J., Visible light driven type II heterogeneous and enhanced their photocatalytic properties: a review nanoscale. **2013**, *5*, 8326–8339.
21. Pelaez, M.; Nolan, N. T.; Pillai, S. C.; Seery, M.K.; Falaras, P.; Kontos, A.G.; Dunlop, P. S. M.; Hamilton, J. W. J.; Byrne, J. A.; O'Shea, K.; Entezari, M. H.; Dionysiou, D. D., A review on the visible light active titanium dioxide photocatalysts for environmental application. *Appl. Catal. B Environ.* **2012**, *125*, 331–349.
22. Coronado, J. M.; Fresno, F.; Hernández-Alonso, M. D.; Portela, R., Design of advanced photocatalytic materials for energy and environmental applications. *Springer*. **2013**.
23. Wu, C.; Shen, L.; Zhang, Y. C.; Huang, Q., Solvothermal synthesis of Cr-doped ZnO nanowires with visible light driven photocatalytic activity. *Mater. Lett.* **2011**, *65*, 1794–1796.
24. Thennarasu, G.; Sivasamy, A., Metal ion doped semiconductor metal oxide nanosphere particles prepared by soft chemical method and its visible light photocatalytic activity in degradation of phenol. *Powder Technol.* **2013**, *250*, 1–12

25. Feng, Z. C., Handbook of Zinc Oxide and Related Materials: Volume two, Devices and Nanoengineering, *CRC Press*. **2012**.
26. Mittal, M.; Sharma, M.; Pandey, O. P., UV–visible light induced photocatalytic studies of Cu doped ZnO nanoparticles prepared by co-precipitation method. *Sol. Energy*. **2014**, *110*, 386–397.
27. Mahmud, S.; Abdullah, M. J.; Putrus, G. A.; Chong, J.; Mohamad, A. K., Nanostructure of ZnO fabricated via French process and its correlation to electrical properties of semiconducting varistors. *Synth. React. Inorg. Met. Org. NanoMet. Chem*. **2003**, *36*, 155–159.
28. Tsuzuki, T.; McCormick, P. G., Mechanochemical synthesis of nanoparticles. *J. Mater. Sci*. **2004**, *39*, 5143–5146.
29. Ao, W.; Li, J.; Yang, H.; Zeng, X.; Ma, X., Mechanochemical synthesis of zinc oxide nanocrystalline. *Powder Technol*. **2006**, *168*, 128–151.
30. Yu, J.; Yu, X., Hydrothermal Synthesis and Photocatalytic Activity of Zinc Oxide Hollow Spheres. *Environ. Sci. Technol*. **2008**, *42*, 4902–4907.
31. Philip, L., Photodegradation of Methyl Parathion and Dichlorvos from Drinking Water with N-Doped TiO₂ under Solar Radiation. *Chem. Eng. J*. **2011**, *172*, 678–688.
32. Birben, N. C.; Paganini, M. C.; Calzab, P.; Bekboleta, M., Photocatalytic degradation of humic acid using a novel photocatalyst: Ce-doped ZnO. *Photochem. Photobiol. Sci*. **2017**, *16*, 24
33. Kuriakose, S.; Satpatib, B.; Mohapatra, S., Enhanced photocatalytic activity of Co doped ZnO nanodisks and nanorods prepared by a facile wet chemical method. *Phys. Chem. Chem. Phys*. **2014**, *16*, 12741
34. Kong, J.; Zhai, H.; Gong, Y.; Li, H.; Wu, D., Journal of Solid State Chemistry Preparation, Characterization of the Ta-Doped ZnO Nanoparticles and Their Photocatalytic Activity under Visible-Light Illumination. *J. Solid State Chem*. **2009**, *182*, 2061–2067.
35. Kanade, K. G.; Kale, B. B.; Baeg, J.; Mi, S.; Wee, C., Self-Assembled Aligned Cu Doped ZnO Nanoparticles for Photocatalytic Hydrogen Production under Visible Light Irradiation. **2007**, *102*, 98–104.

36. Vignesh, K.; Suganthi, A.; Rajarajan, M.; Sara, S. A., Photocatalytic Activity of AgI Sensitized ZnO Nanoparticles under Visible Light Irradiation. *Powder Technol.* **2012**, *224*, 331–337.
37. Mahmood, M. A.; Baruah, S.; Dutta, J., Enhanced Visible Light Photocatalysis by Manganese Doping or Rapid Crystallization with ZnO Nanoparticles. *Mater. Chem. Phys.* **2011**, *130*, 531–535.
38. Liu, S.; Li, C.; Yu, J.; Xiang, Q., Improved Visible-Light Photocatalytic Activity of Porous Carbon Self-Doped. **2011**, 2533–2541.
39. Judith, P.; Espitia, P., Zinc Oxide Nanoparticles : Synthesis, Antimicrobial Activity and Food Packaging Applications. **2012**, 1447–1464.
40. Shirzad-siboni, M.; Jonidi-jafari, A.; Farzadkia, M.; Esra, A.; Gholami, M., Enhancement of Photocatalytic Activity of Cu-Doped ZnO Nanorods for the Degradation of an Insecticide : Kinetics and Reaction Pathways. **2017**, *186*.
41. Zhang, G.; Shen, X.; Yang, Y., Facile Synthesis of Monodisperse Porous ZnO Spheres by a Soluble Starch-Assisted Method and Their Photocatalytic Activity. *J. Phys. Chem. C.* **2011**, *115*, 7145–7152.
42. Pan, C.; Dong, L.; Qu, B.; Wang, J., Facile Synthesis and Enhanced Photocatalytic Performance of 3D ZnO Hierarchical Structures. *J. Nanosci. Nanotechnol.* **2011**, *11*, 5042–5048.
43. Lepot, N.; Van Bael, M. K.; Van den Rul, H.; D’Haen, J.; Peeters, R.; Franco, D.; Mullens, J., Synthesis of ZnO Nanorods from Aqueous Solution. *Mater. Lett.* **2007**, *61*, 2624–2627.
44. Fu, M.; Li, Y.; Wu, S.; Lu, P.; Liu, J.; Dong, F., Sol-Gel Preparation and Enhanced Photocatalytic Performance of Cu-Doped ZnO Nanoparticles. *Appl. Surf. Sci.* **2011**, *258*, 1587–1591.
45. Mohan, R.; Krishnamoorthy, K.; Kim, S. J., Enhanced Photocatalytic Activity of Cu-Doped ZnO Nanorods. *Solid State Commun.* **2012**, *152*, 375–380.

46. Rather, R. A.; Singh, S.; Pal, B., Visible and Direct Sunlight Induced H₂ Production from Water by Plasmonic Ag-TiO₂ Nanorods Hybrid Interface. *Sol. Energy Mater. Sol. Cells.* **2017**, *160*, 463–469.
47. Lam, S. M.; Abdullah, A. Z; Mohamed, A. R., Degradation of wastewaters containing organic dyes photocatalysed by zinc oxide: a review, *Desalin. Water treat.* **2012**, *41*, 131-169.

PLAGIARISM CERTIFICATE

ORIGINALITY REPORT

% **15**
SIMILARITY INDEX

% **7**
INTERNET SOURCES

% **14**
PUBLICATIONS

% **0**
STUDENT PAPERS

PRIMARY SOURCES

1 Samadi, Morasae, Mohammad Zirak, Amene Naseri, Elham Khorashadizade, and Alireza Z. Moshfegh. "Recent progress on doped ZnO nanostructures for visible-light photocatalysis", *Thin Solid Films*, 2016. %**2**
Publication

2 doria.fi %**1**
Internet Source

3 He, Yiming, Jun Cai, Lihong Zhang, Xiaoxing Wang, Hongjun Lin, Botao Teng, Leihong Zhao, Weizheng Weng, Huilin Wan, and Maohong Fan. "Comparing Two New Composite Photocatalysts, t-LaVO₄/g-C₃N₄ and m-LaVO₄/g-C₃N₄, for Their Structures and Performances", *Industrial & Engineering Chemistry Research*, 2014. <%**1**
Publication

4 Vignesh, K.. "Photocatalytic activity of AgI sensitized ZnO nanoparticles under visible light irradiation", *Powder Technology*, 201207 <%**1**
Publication